Science of the Total Environment 755 (2021) 143170

Contents lists available at ScienceDirect

Science of the Total Environment

journal homepage: www.elsevier.com/locate/scitotenv

# UV degradation of natural and synthetic microfibers causes fragmentation and release of polymer degradation products and chemical additives

Lisbet Sørensen [a,*], Anette Synnøve Groven [b], Ingrid Alver Hovsbakken [b], Oihane Del Puerto [a], Daniel F. Krause [a], Antonio Sarno [a], Andy M. Booth [a]

[a] SINTEF Ocean AS, Trondheim, Norway
[b] Norwegian University of Science and Technology (NTNU), Trondheim, Norway

## HIGHLIGHTS

- Both synthetic and natural (wool) textile fibers are susceptible to UV degradation.
- Polyamide and polyester fibers observed formation of micrometer-sized holes.
- Polyester and wool fibers fragmented in less than 2 months
- Degradation products and chemical additives leached from all fibers.

## GRAPHICAL ABSTRACT

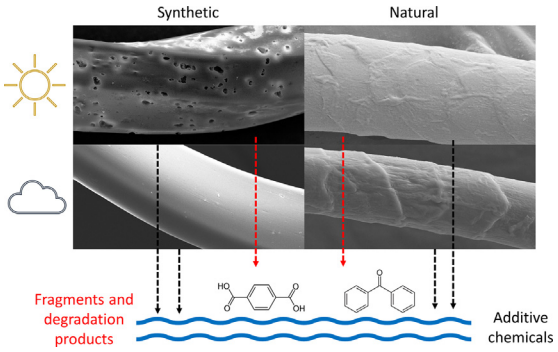


## ARTICLE INFO

*Article history:*
Received 18 September 2020
Received in revised form 13 October 2020
Accepted 14 October 2020
Available online 22 October 2020

Editor: Damia Barcelo

*Keywords:*
Microplastic fibers
Synthetic textiles
Wool
Polyester
Polyamide
Non-target screening
Leaching

## ABSTRACT

A high proportion of the total microplastic (MP) load in the marine environment has been identified as microfibers (MFs), with polyester (PET) and polyamide (PA) typically found in the highest abundance. The potential for negative environmental impacts from MPs may be dependent on their degree of degradation in the environment, which is influenced by both intrinsic properties (polymer type, density, size, additive chemicals) and extrinsic environmental parameters. Most polymer products break down slowly through a combination of environmental processes, but UV degradation can be a significant source of degradation. The current study aimed to investigate the effect of UV irradiance on the degradation of natural (wool) and synthetic (PET and PA) MFs. Degradation of MFs was conducted in seawater under environmentally relevant accelerated exposure conditions using simulated sunlight. After 56 days of UV exposure, PA primarily exhibited changes in surface morphology with no significant fragmentation observed. PET and wool fibers exhibited both changes in surface morphology and fragmentation into smaller particles. A range of molecular degradation products were identified in seawater leachates after UV exposure, with increasing abundance over the duration of the experiment. Furthermore, a variety of additive chemicals were shown to leach from the MFs into seawater. While some of these chemicals were also susceptible to UV degradation and some are expected to biodegrade rapidly, others may be persistent and contribute to the overall load of chemical pollution in the marine environment.



## 1. Introduction

In the 1970s, synthetic fiber densities up to $10^5$ $m^{-3}$ were reported in North Sea water samples (Buchanan, 1971) and microplastic fibers (MPFs) are often identified as the most dominant type of microplastic

* Corresponding author.
*E-mail address:* lisbet.sorensen@sintef.no (L. Sørensen).

https://doi.org/10.1016/j.scitotenv.2020.143170

(MP) in both the water column (Browne et al., 2011; Thompson et al., 2004) and sediments (Claessens et al., 2011; Mathalon and Hill, 2014). For example, 80% of MP found in the Arctic Central Basin were MPFs (Kanhai et al., 2018). In a study of MP pollution in Arctic waters, a staggering 95% of MP were classified as fibers (Lusher et al., 2015), with polyester (PET) and polyamide (PA) particles were found in the highest abundance, both with a detection frequency of 15% (Lusher et al., 2015). PET and PA fibers were also quantified in similar frequencies in Arctic sea ice, indicating the water column may be the main source of MP found in sea ice (Obbard et al., 2014).

Textile washing has been identified as a major source of MPFs to the environment (Browne et al., 2011), although the level of MPF release is dependent on factors such as polymer type, fabric type (including fiber, yarn, weave and finishing), type of washing machine, washing program and type of detergent (De Falco et al., 2018; Hartline et al., 2016; Napper and Thompson, 2016; Salvador Cesa et al., 2017). An early study estimated one garment can shed >1900 fibers per wash, leading to a MPF concentration of >100 fibers/L of effluent (Browne et al., 2011), with polyester fleece has been demonstrated to release the most fibers (Carney Almroth et al., 2018). More recent studies have calculated an average household wash of polyester clothing (5–6 kg) releases between 500,000-6,000,000 fibers (De Falco et al., 2018; Napper and Thompson, 2016). However, direct comparison of fiber release studies is difficult due to a lack of standard methods for testing fiber release and for reporting data (Carney Almroth et al., 2018; Cesa et al., 2020; De Falco et al., 2018; Freeman et al., 2020; Frias and Nash, 2019).

While wastewater treatment plants (WWTPs) are not specifically designed to retain MPs (Ben-David et al., 2021; Freeman et al., 2020; Habib et al., 1998; Nerland et al., 2014), they have been demonstrated to remove up to 99% of MPs in the primary and secondary treatment steps (Ben-David et al., 2021; Freeman et al., 2020; Salvador Cesa et al., 2017). Despite the efficient removal, annual emissions from just one WWTP have been estimated to correspond to up to $6.7 \times 10^{12}$ MP particles (Leslie et al., 2017). Importantly, MPFs are one of the MP types least effectively retained in WWTPs and can represent >90% of the total MP load in effluents (Ben-David et al., 2021; Lares et al., 2018).

The potential for negative environmental consequences from MPs may be dependent on their degree of degradation and transformation in the environment, which is influenced by both intrinsic properties (polymer type, density, size, additive chemicals) and extrinsic environmental parameters (UV irradiation, biofouling). Most polymer products break down very slowly through a combination of photodegradation, oxidation and mechanical abrasion, with the major degradation step being UV-initiated oxidation (Andrady, 2015; Booth et al., 2018). However, there is very limited data on the rates at which different polymers degrade and fragment under varying environmental conditions (Andrady, 2015; Booth et al., 2018).

The negative effects of MPFs on organisms has been less extensively studied than those associated with spherical and irregular shaped MPs (Cole et al., 2019; Cole et al., 2013; Jemec et al., 2016), representing a significant knowledge gap considering they often represent a high proportion of the total MP in an environmental matrix. Focus has also been given recently to the potential effects of additive and production chemicals leaching from plastic into water (Zimmermann et al., 2019). In addition to acute effects, plastic leachates have been shown to induce effects such as oxidative stress, cytotoxicity, estrogenicity, and antiandrogenicity (Capolupo et al., 2020; Hermabessiere et al., 2017; Rummel et al., 2019; Zimmermann et al., 2019). Chemicals are added to polymers to provide products with specific functionalities and durability. For this purpose, softeners and dyes are commonly added to textile polymers, but also antioxidants, UV stabilizers, antimicrobials and even flame retardants are routinely added depending on the intended product applications (Hermabessiere et al., 2017).

A recent study demonstrated the presence of a large number and variety of additive chemicals, synthesis by-products and residues in textilefibers (Sait et al., 2020). When released to aqueous environments, several of these compounds would be expected to leach from the fibers depending on their solubility. Furthermore, degradation of MP has been shown to effect interaction with chemical pollutants already present in the environment (Zhang et al., 2018), however, the effect of UV-exposure on the extent of additive leaching has not previously been quantified. Finally, UV-degradation may cause formation of water-soluble polymer degradation products, but this process has also yet to be investigated for textile polymers.

The current study investigated the UV degradation of PET and PA relative to a natural wool microfiber (MFs). The study also tested the hypothesis that fiber degradation increases the available surface area and facilities increased additive chemical leaching. Degradation of the MFs was conducted in seawater under environmentally relevant accelerated exposure conditions using simulated sunlight, while control samples were incubated in the dark. The leaching of organic additive chemicals and release of UV degradation products from all fiber types was studied as a function of UV exposure time. Fragmentation and physical changes to the fiber surfaces were studied using light and scanning electron microscopy, while identification and quantification of additive chemical release and degradation product generation was achieved using a suite of analytical chemical techniques.

## 2. Materials and methods

### 2.1. Chemicals and materials

Analytical grade dichloromethane (DCM), hydrochloric acid (HCl, 37%), sodium sulphate ($Na_2SO_4$) and ammonium formate ($NH_4HCO_2$, 10 M) were purchased from Merck and Sigma-Aldrich. HPLC-grade acetonitrile and formic acid were purchased from Fisher Chemicals. Reference chemicals and deuterated standards were supplied by Chiron AS (Trondheim, Norway) and Sigma-Aldrich.

### 2.2. Preparation of microfibers

White polyester (PET), polyamide (PA) and wool yarns were kindly provided by commercial textile producers (details in SI; Table S1). Microfibers (MFs) from the different yarns were prepared with minor modifications according to Cole (2016). Briefly, segments of yarn were fixed at −80 °C using glycol frozen section medium (colorless Richard-Allan Scientific™ Neg-50™) before being sectioned to ~2 mm using a scalpel. The sectioned MFs were rinsed with MilliQ® water to remove glycol, isolated by filtration (0.45 μm HAWP cellulose filters, MF-Millipore) and dried over night at 40 °C.

### 2.3. Laboratory UV exposure

Samples of the MFs (100 mg each, corresponding to ~180,000 PET, ~114,000 PA and 63,000 wool particles and a surface area of respectively 227, 199 and 137 $cm^2$) were placed in 35 mL quartz glass tubes filled with ~32 mL sterile filtered (0.22 μm, Sterivex®) natural seawater obtained from a depth of 90 m in Trondheimsfjorden. UV exposure experiments were performed using an Atlas Suntest CPS+ instrument fitted with a Xenon lamp (1500 W) and sunlight filter, with intensity regulated using the emission range between 300 and 400 nm. Irradiation was conducted at an intensity of 65 $W/m^2$, while the temperature in the exposure chamber was maintained at 24 ± 3 °C. For each MF type, three replicate samples were subject to UV exposure and one control sample was kept in the dark at room temperature (20 ± 1 °C). The difference in exposure temperatures between the UV and dark controls is the result of the heat generated by the UV lamp which raised the temperature slightly above room temperature. Seawater blank controls were subject to treatment either as UV-exposed or dark control samples. To ensure homogenous exposure conditions, samples and controls were gently agitated daily for the first two weeks, which was reduced to bi-weekly for the remaining exposure period. Sampling was conducted

after 14, 28 and 56 days. Using the equations proposed by Gewert et al. (2018), the irradiation level and these exposure periods correspond to simulated environmental exposure periods under European mean irradiance of 133 (~4.5 months), 266 (~9 months) and 531 days (~1.5 years), respectively (see SI for calculation). At each time point, the entire sample was decanted from the quartz tube and MFs isolated by filtration (40 μm, Corning® sterile nylon cell strainer) followed by thorough rinsing with MilliQ® water to remove salts. At 14 and 28 days, a sub-sample of MFs (<10 mg) was taken from each filter, dried over night at 40 °C and stored in the dark until further processing. The remaining MFs on the filters were transferred back to the exposure vessels and fresh sterile filtered seawater (~32 mL) was added to continue the exposure. At 56 days, all of the MFs in each sample (>80 mg) were collected. At all sampling points the seawater filtrate from the 40 μm filters was collected and filtered a second time (0.45 μm HAWP cellulose filters, MF-Millipore) to remove any smaller fiber fragments. The final filtrate was then acidified (pH <2) using HCl (15% v/v) and stored in the dark at 4 °C prior to extraction and analysis.

### 2.4. Physical characterization of MPFs

All light microscopy was performed using a Nikon Eclipse 80i microscope and post-processed in ImageJ® (Schneider et al., 2012). The scale was set according to the objective lens used and calibrated using a stage micrometer slide. The length distributions of UV-exposed and control fibers were determined by freehand tracing of the fibers in ImageJ® using a Wacom digitizing tablet. Changes in the surface morphology of pristine, UV-exposed and dark control fiber samples were investigated by scanning electron microscopy (SEM). Fibers were thinly coated (~18.4 nm) with a layer of gold via low vacuum sputtering (Quorum SC7620 Mini Sputter Coater) to minimize charge build-up. A tabletop SEM (Jeol JCM-6000Plus) was first applied to screen for visible changes, followed by detailed imaging using a Zeiss Field Emission SEM (Ultra 55 Limited Edition or Supra 55VP). Images were captured at 4 different magnifications (100×, 500×, 2000× and 10,000×) using a 10 mm working distance and a 2–10 kV accelerating voltage.

### 2.5. Non-target and target screening for degradation products and leached additives using GC–MS

Non-target organic chemical profiling was conducted on solvent extracts produced from both the pristine MFs and the seawater leachates. To determine the organic compounds present in the pristine PET, PA and wool materials, samples of each fiber type (100 mg) were extracted with 4 mL DCM ($n = 3$) by ultrasonication for 30 min at room temperature. Solvent extracts were filtered (Whatman GF/F) to remove the MFs and volume adjusted by gentle evaporation at 37 °C under a stream of $N_2$ to approximately 500 μL prior to gas chromatography–mass spectrometry (GC–MS) analysis. Seawater filtrates containing leached additives and soluble degradation products (~35 mL) were spiked with surrogate internal standards (250.8 ng naphthalene-*d*8, 50 ng phenanthrene-*d*10, 48.6 ng chrysene-*d*12, 50.8 ng perylene-*d*12), extracted three times using dichloromethane (1 × 10 mL and 2 × 5 mL), the organic extract dried using $Na_2SO_4$ and finally the volume adjusted to approximately 400 μL. A recovery standard (100 ng fluorene-*d*10) was added before GC–MS analysis.

Non-target screening of the MF and seawater leachate extracts was performed using an Agilent 7890A GC gas chromatograph (GC) coupled to an Agilent 5975C MS. Samples (1 μL) were introduced at 250 °C in pulsed splitless mode. Separation was achieved using a Zebron ZB-1MS column (30 m length, 0.25 μm film thickness and 0.25 mm internal diameter). The carrier gas was helium at a constant flow of 1.1 mL/min. The column oven temperature was programmed at 90 °C (1 min), ramped by 5 °C/min until 320 °C (10 min hold). The transfer line temperature was 300 °C, the ion source temperature was 230 °C and the quadrupole temperature 150 °C. The ion source was operated in fullscan mode (50–500 *mz*) at 70 eV, with a solvent delay of 5 min. To quantify selected additive compounds in the MF and leachate extracts, target analysis was also performed on the same extracts as above. To improve detection limits, the MS was operated in selected ion monitoring (SIM) mode, monitoring the three most abundant ions for each analyte (Table S2, SI). Target analytes were quantified by quadratic regression of a 10-level calibration curve (0.1–1000 ng/mL) after normalization to an internal standard (fluorene-*d*10).

### 2.6. PET degradation products by LC-UV/LC-MS/MS

Ethylene glycol and terephthalic acid degradation products produced from UV exposure of PET were quantified in seawater samples using a combination of LC-UV and LC-MS/MS analysis. Ethylene glycol was first derivatized with benzoyl chloride as previously described by Imbert et al. (2014). Derivatization was accomplished by adding 50 μL of the seawater sample to 100 μL 4 M NaOH, 50 μL benzoyl chloride and 50 μL MilliQ water. The reaction was vortexed and incubated at room temperature for 5 min, before quenching by addition of 50 μL 10% glycine and a further incubation for 3 min at room temperature. The resulting dibenzoyl derivate was then extracted with 1 mL pentane. Phase separation was accomplished by centrifugation at 10000 x*g* for 5 min, after which the organic phase was evaporated under nitrogen at 50 °C. The dried extract was dissolved in 800 μL of 10 mM ammonium formate (pH 2.8) in 50% acetonitrile. Derivatized samples were diluted 500-fold prior to analysis. Terephthalic acid was analyzed directly by diluting samples 100-fold prior to analysis, without the need for derivatization.

Samples were analyzed on an Agilent 1260 HPLC system equipped with a variable wavelength detector coupled to a 4670 triple quadrupole mass spectrometer (MS) equipped with an electrospray ion source. The HPLC column (ZORBAX Eclipse Plus C18 2.1 × 50 mm, 1.7 μm particle size, Agilent Technologies) was kept at 25 °C and the injection volume was 10 μL. The mobile phase consisted of 10 mM ammonium formate pH 2.8 (A) and acetonitrile containing 0.1% formic acid (B). The 7.5 min HPLC program for ethylene glycol was as follows: start at 10% B, ramp to 90% B by 3 min, hold until 3.5 min, and ramp to 10% B by 3.6 min. The ethylene glycol derivate was detected by MS using the following mass transitions in positive ionization mode: *m/z* 271.1 → 149 (quantifier) and *m/z* 271 → 105.1 (qualifier). The 6.5 min HPLC program for terephthalic acid was as follows: start at 10% B, ramp to 90% B by 2 min, hold until 2.5 min, and ramp to 10% B by 2.6 min. Terephthalic acid was detected by UV absorption at 254 nm and peak identity was confirmed by MS in negative mode using *m/z* 165 → 121.1.

### 2.7. Data analysis and statistical treatment

For non-target analysis, GC chromatograms and mass spectra were recorded in ChemStation software and MassHunter Unknowns Analysis software was applied to the raw data files for deconvolution and tentative identification of analytes. Output files were exported to .csv format for further processing using R (R Development Core Team, 2008). In R, compounds were filtered based on their presence in at least 2 of 3 replicates and when >80% match to NIST 2017 library mass spectra was obtained. A Shapiro-Wilks test revealed a non-normal distribution of fiber length data, and thus a Kruskal-Wallis test was performed to investigate significant length changes for each fiber type (PET, PA, wool), followed by Dunn's multiple comparison test.

## 3. Results and discussion

### 3.1. Physical degradation of fibers following UV exposure

After UV exposure, both polyamide (PA) and polyester (PET) fibers showed signs of degradation at the fiber surface when investigated by SEM (Fig. 1). No surface changes were observed in dark control samples

at any of the time points studied (up to 56 days). Both PA and PET fibers clearly exhibited the formation of holes or pitting in their surfaces, although this was much more pronounced in the PA than the PET fibers. These changes in surface morphology are consistent with observations of MP fibers found in sun-exposed environmental compartments (Sathish et al., 2019). For both polymers, the surface changes could be observed already after 14 days and there was no clear increase in surface degradation with increasing exposure time up to 56 days. A different form of degradation was observed for wool fibers, where the surface fibrils appeared to be smoothed during UV exposure. In contrast to the synthetic PA and PET fibers, the surface degradation became more pronounced over the 56 day duration of the experiment.

PA is typically seen as resistant to environmental degradation (Tokiwa et al., 2009). However, embrittlement of UV- and environmentally exposed PA films have previously been demonstrated (Achhammer et al., 1951). Early studies showed that increased humidity provoked more significant UV degradation of both PA and PET, indicating that UV degradation of polymers in surface waters will be more pronounced than in dry environments (Lock and Frank, 1973). While cracking or microcracking is often described in UV degradation of PET, the formation of small holes observed on the surface of PET MPFs has not previously reported in laboratory UV degradation studies (Armstrong et al., 1995). Small holes have been observed on the surface of polycarbonate films after hydrolytic degradation studies (Chandure et al., 2014), as well as in fibers having undergone degradation in the environment (Sathish et al., 2019), suggesting hydrolysis may be occurring concurrently with UV degradation in the current study.

Although surface degradation was more pronounced for PA fibers than PET fibers, no significant ($p > 0.05$) fragmentation was observed for PA fibers over the 56 day exposure period (Fig. 2). In contrast, PET fibers exhibited only minor changes to their surface but underwent a significant ($p < 0.05$) degree of fragmentation. Changes in fiber length distribution decreased from a median value of 3115 μm prior to exposure (day 0) to 2492 μm after 14 days ($p < 0.05$), 1249 μm after 28 days ($p < 0.001$) and 257 μm after 56 days ($p < 0.0001$) of UV exposure. Wool fibers did not significantly ($p > 0.05$) fragment over the first 28 days of UV exposure, but the median length had decreased from 3156 (day 0) to 1292 μm after 56 days ($p < 0.0001$).

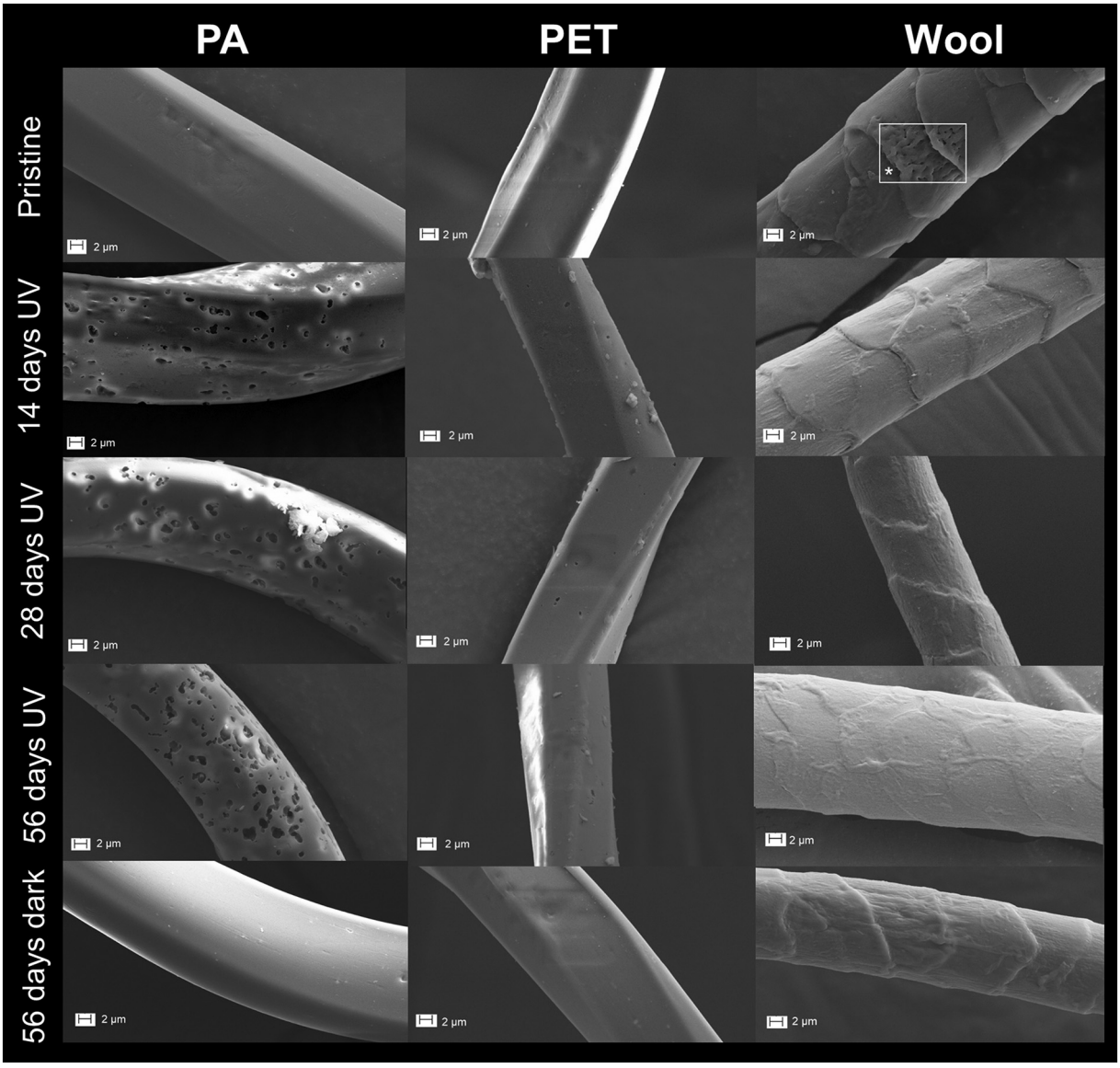


**Fig. 1.** SEM images of PA, PET and wool fibers exposed to UV for 14, 28 and 56 days, compared to pristine and dark control samples (kept in seawater for 56 days). The area marked * on the pristine wool sample reflects damage caused by imaging at 10 kV, and is not degradation.

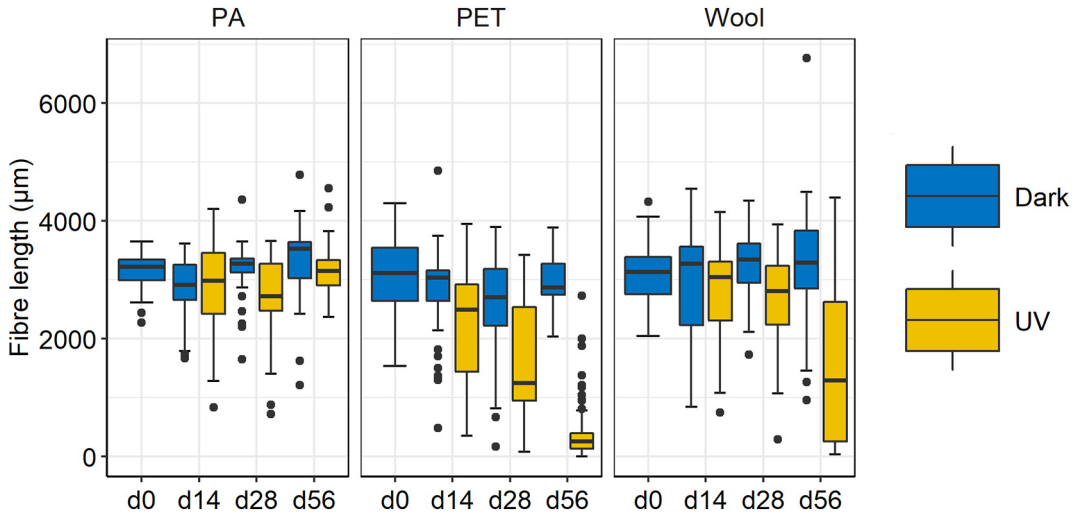


**Fig. 2.** Length of PA, PET and wool fibers in UV exposed and dark control samples at days 14, 28 and 56 compared to pristine (d0) samples. Boxplots: median and 25 to 75 percentiles; bars: minima and maxima; black dots represent outliers.

While it appears likely that UV degradation of PET and wool fibers contributes to fragmentation and the formation of smaller fibers, it is unclear whether this is the case with PA. The observed 'holes' on the fiber surface may be formed from a purely chemical degradation of the surface polymer, primarily resulting in the release of monomers and degradation products. However, it could also be the case that tiny PA fragments released from the PA fiber surface during UV degradation. From the shape and size of the holes (<5 μm diameter, Fig. 1), it is suggested that any such fragments may be in the nanoparticle range. Due to the methods employed in the current study, assessment of nano-sized fragmentation products was not possible, but this should be the focus of future studies given the potential for increased impacts from particles of that size.

The fragmentation of textile MFs appears critical for altering their bioavailability, primarily by reducing the particle size and making them available for ingestion by smaller organisms such as zooplankton (Sørensen et al., 2020). In contrast, changes in surface morphology may alter how microbiota interact with MFs leading to differences in microbial biofouling and colonization. It is also suggested that changes in surface morphology and fragmentation may both influence how MFs are transported in the water column and their general environmental fate and behavior.

### 3.2. Formation and release of polymer degradation products

It has been suggested that UV degradation of PA starts by breaking of the C—N bond of the amide group, forming molecules of the same unit of chemical structure (Achhammer et al., 1951). In the current study, non-target analysis (fullscan GC–MS) of seawater surrounding UV-exposed PA fibers indicated the formation and release of alkylated amides (Table S2, Fig. S1, SI). Only trace levels were present in dark controls and seawater control samples. Caprolactam, the synthesis precursor of nylon 6, was found in both UV and dark controls. Concentrations determined after 14 days represented maximum levels, with no further leaching of caprolactam was observed after 14 days. The results suggest caprolactam in the seawater derives entirely from the leaching of residues present in the PA fibers from the synthesis process, rather than being a degradation product formed from UV exposure. Some of the other tentatively identified compounds in the PA seawater leachates had a structure unlikely to be formed from degradation of PA polymer. It is hypothesized that these chemicals were already present in the fibers as synthesis by-products and that they are released in a similar way to caprolactam. However, concentrations continued to increase from day 14 to day 56, which may reflect an increasing surface area for leaching to occur due to the formation of pitting from the UV degradation process.

UV degradation of PET has been proposed to occur via chain scission leading to the generation of carboxyl end groups followed by the formation of mono- and dihydroxyterephthalates, and aldehydes (Fechine et al., 2004). In the current study, non-target analysis revealed the presence of several tentatively identified (fullscan GC–MS) degradation products of PET in the seawater leachates after 14 days (Table S3, Fig. S2, SI). In the order of relative abundance, these included: 1,2-ethanediol monobenzoate, terephthalic acid, 4-acetylbenzoic acid, benzoic acid, 4-methylbenzoic acid, phenacyl formate, vinyl benzoate, diethylene glycol dibenzoate and 4-ethylbenzoic acid. These compounds correspond to the breaking of C—C or C—O bonds in the PET polymer backbone, with the exception of 4-methyl- and 4-ethylbenzoic acid, which must be formed through re-arrangement. All compounds showed an exponential increase in formation over the course of the experiment, suggesting a continued production as the UV degradation process proceeded (Table S3, Fig. S2, SI). Only trace levels of these chemicals were detected in dark controls and seawater control samples. By use of target analysis, the formation of terephthalic acid was verified and quantified, and additionally the fragment ethylene glycol could be traced quantitatively over time – which confirmed the trend observed based on the non-target analysis (Fig. 3). This shows that the original constituent chemicals used in the production of PET are also formed during UV degradation, together with a suite of other products.

In seawater samples from UV-exposure wool fibers, several sulfurous compounds (cyclic octaatomic sulfur, lenthionine, hexathiane and hexathiepane) were tentatively identified (Table S3, Fig. S3, SI). The concentration increased over time and only trace amounts were observed in dark controls and seawater controls, suggesting a direct link to the UV exposure. It is hypothesized that these compounds are formed through degradation of the amino acid cysteine, which is found in wool, and known to degrade stepwise to sulfur. Empirically, wool fibers were observed to become yellow and a characteristic odor typical of sulfurous chemicals was detected when sampling. Interestingly, benzoic acid was also found in the UV-exposed wool leachates. One possible explanation for the presence of this chemical is the common use of a PET polymer coating on the surface of the wool fibers to increase the durability of textiles. However, target analysis for the PET degradation products terephthalic acid and ethylene glycol did not verify this. Furthermore, no other PET degradation products were observed in the wool UV leachates. Therefore, the observed presence of benzoic acid is

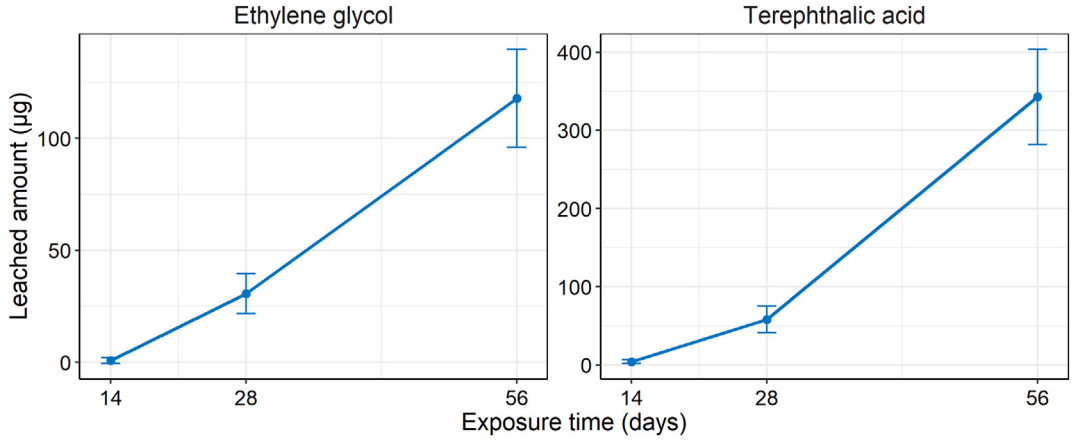


**Fig. 3.** Formation of ethylene glycol and terephthalic acid (µg) degradation products as a function of time during UV exposure of PET fibers.

hypothesized to be caused by its use at some point in the fiber production process.

### 3.3. Leaching of additive chemicals

In addition to studying the formation and release of degradation products, the leaching of additive chemicals associated with each of the different MF materials was also profiled and quantified. In the first step, additive chemicals present in the MF leachates at days 14, 28 and 56 were investigated using non-target (fullscan) GC–MS analysis and tentatively identified by mass spectral matching to the NIST 2017 spectra database (Table S4, Fig. S4, SI). While the tentatively identified additive chemicals were specific to individual MF types in many cases, some additives (e.g. benzophenone) were associated with multiple MFs. Furthermore, UV stabilizers (e.g. benzophenone, benzotriazoles) were only observed in the dark controls and not in the corresponding UV-exposed MF leachates. This is consistent with UV stabilizers degrading under UV exposure, absorbing potentially damaging wavelengths in order to protect the polymer matrix. Other additive chemicals with different functions (i.e. other than UV stabilization) were primarily observed in UV-exposed samples and not in the corresponding dark controls, suggesting that the degradation process facilitates their increased released and also that the chemicals are more resistant to UV degradation than UV stabilizers. In the second step, reference chemical standards corresponding to a selection of the identified additives were used in conjunction with specifically developed SIM-based targeted GC–MS analysis to (i) confirm the tentative identification, (ii) quantify additive leaching over time and (ii) determine additive concentrations in solvent extracts of the pure MF materials.

As plasticizers are common laboratory contaminants, they were not studied in the seawater leachates, as it was not possible to ensure the source of these chemicals in the leachates came entirely from the MFs. However, we could unambiguously identify and quantify a number of phthalates, bisphenol A (BPA), *n*-butylbenzenesulfonamide (nBBSA) and *p-tert*-octylphenol (ptOCP) in solvent extracts of the MFs (Fig. S5, SI). Many of these chemicals were identified in all MF types, but some were material specific. Bis(2-ethylhexyl) phthalate (BEHP) was the phthalate present in highest extractable concentration overall, followed by diethyl phthalate (DEP) and benzyl butyl phthalate (BBP). Wool fibers typically had the highest levels of plasticizers, followed by PA. Several organophosphorus compounds were also quantified in MF extracts; with the highest overall concentrations observed for triphenyl phosphate (TPhP), followed by tris(2-chloroethyl) phosphate (TCEP) and tripropyl phosphate (TPP). Other notable additives present in the MF materials included benzophenone, benzothiazole, phthalide and phthalimide. Generally, the lowest levels of additives were seen in PET fibers, and the highest in wool fibers. TPP and phthalide could not be quantified in the wool extracts, but this may be due to confounding co-elution in the GC chromatograms (Fig. S6, SI). The relatively high levels of additives in wool fibers have previously been described, and are likely due to surface treatment of the raw-material to improve functionality for use in textile production (Sait et al., 2020). Benzothiazole is most commonly used as a vulcanizer in the manufacture of rubber, and known to leach in high quantities from rubber to water (Capolupo et al., 2020; Dsikowitzky et al., 2014), Although the use of benzothiazole in polymer production is not widely known, the presence of benzothiazole in a large number of consumer textiles has recently been demonstrated (Avagyan et al., 2015; Liu et al., 2017) and the release of this and other compounds during domestic washing has been reported (Luongo et al., 2016).

Of the additive compounds found in the MFs (omitting plasticizers), seven were also quantifiable in the seawater leachates (Fig. 4). As observed from the non-target analysis, the benzophenone (UV stabilizer) concentration in seawater from PA, PET and wool fibers in dark controls increased exponentially over the duration of the exposure, while concentrations in UV-exposed samples remained at background levels. In contrast, phthalide, phthalimide, TPP, TPhP and TCEP concentrations increased over time to a greater extent in the UV-exposed samples compared to the dark control samples (Fig. 4). These compounds are not expected to UV degrade rapidly and their increased concentrations confirms the hypothesis that fiber degradation increases the available surface area and facilities increased additive chemical leaching. Benzothiazole exhibited a more unique behavior, with concentrations increasing beyond the background (seawater control) levels in both UV exposed and dark controls. While benzothiazole concentrations were higher in UV-exposed wool samples than in the corresponding dark controls, the opposite trend was observed for PA and PET. While it is not clear what causes this difference, it is suggested that differences in the level and duration of surface morphology changes may play a role. For the wool fibers, an increasing surface degradation was observed over the whole 56 day UV exposure period (Fig. 1), which may facilitate continuous leaching of benzothiazole at a rate that is higher than its loss from the system due to UV degradation. In contrast, changes in PA and PET surface morphology due to UV degradation seemed to reach a maximum after 14 days (Fig. 1), suggesting no additional surface is made available for continued leaching over the course of the experiment. As a result, UV degradation of leached benzothiazole might be occurring at a rate that is faster than the leaching process in these two MF materials.

Interestingly, the relative concentrations of additive chemicals quantified in the UV-exposed leachates and MF extracts were not comparable across the different fiber types. While high concentrations of all

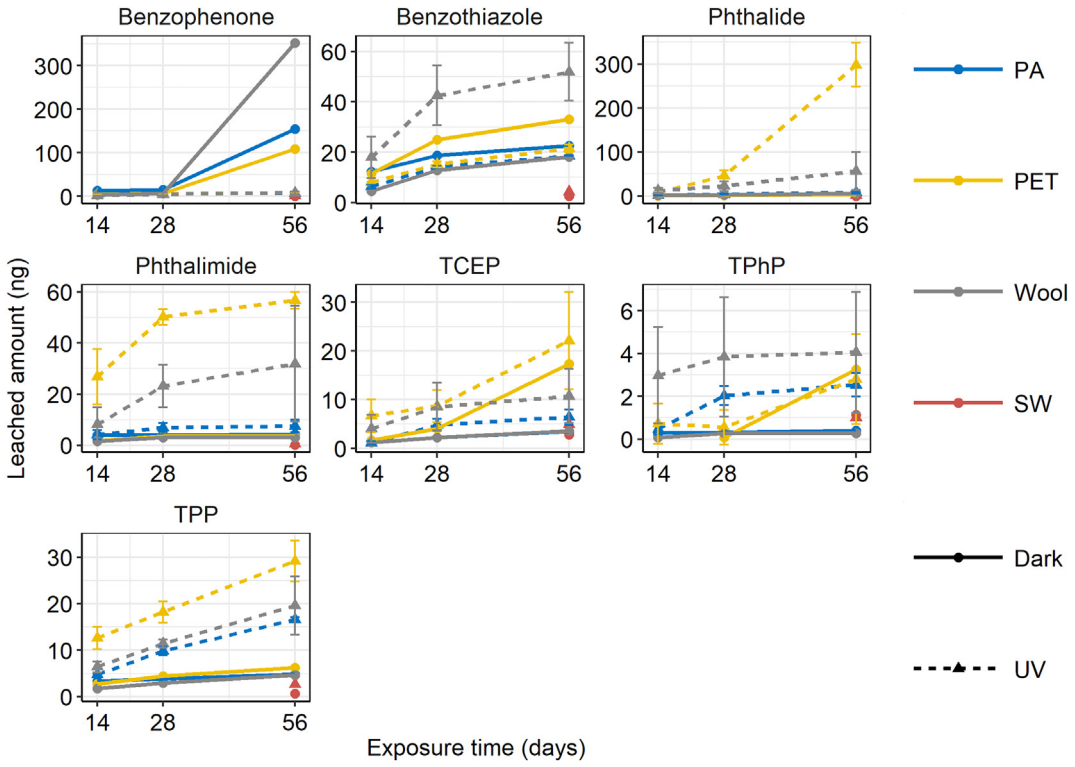


**Fig. 4.** Additives leaching from fibers over time. Presented as the cumulative leached amount (ng) for each exposure. Error bars denote standard deviation ($n = 3$).

additive chemicals were typically determined in the PA fibers (Fig. S5), their corresponding leachate concentrations were comparably low (Fig. 4). Conversely, additive concentrations in the PET and (to some degree) the wool fibers were lower than PA, but where present at higher concentrations in the corresponding leachates. Possible explanations for this may be differences in affinity of the additives to the different polymers, or in how the additives are incorporated in the materials. Additionally, the differences in physical degradation of the different fiber types may cause increased potential for leaching of additives from fibers where the surface degrades (wool) or the fibers fragment increasingly over time (wool and PET). Also, comparing the levels of extractable additives from MFs with the maximum observed concentration in respective leachates (made from 0.1 g MF) – it is evident that prolonged leaching in seawater, particularly under UV, causes more additive chemical to be released than during the solvent extraction process, possibly due to a combination of the polarity of the chemicals relative to the solvent and that the solvent did not cause changes to the surface morphology through dissolution or degradation of the fibers. Differences in relative concentrations of chemicals in the leachates compared to the MFs may be due to a combination of differences in polymer affinity, water solubility and degradation once released to water.

Chemical additives used as UV stabilizers were observed to degrade under UV exposure following their release from MFs, suggesting they would rapidly be removed in aquatic environments with high sunlight levels. While other additives leaching from the MFs appeared resistant to UV degradation, other degradation processes may play an important role in their fate and persistence in the natural aquatic environments. For example, the current study was performed under sterile conditions, but biotic degradation could also be expected to impact additive chemicals leaching from fibers in the environment. However, none of the additive chemicals quantified in any of the MF leachates were estimated to be readily biodegradable according to the US EPA EpiSuite™ software (US EPA, 2012), suggesting potential for persistence and accumulation in the environment. In contrast, all of the tentatively identified polymer degradation products are expected to biodegrade rapidly in the environment according to the same assessment. Knowing that MP leachates may be significantly toxic (Capolupo et al., 2020) and that model estimates indicate a high proportion of additive chemicals may be considered persistent, the role of MFs and other MPs as a potential source of chemical pollution in aquatic environments should be given increased attention in future work and considered within MP risk assessment and future mitigation actions.

## 4. Conclusions

In the current study, it was shown that once released to the aquatic environment, both synthetic and natural fibers may UV-degrade and release a complex mixture of additive chemicals, chemical residues from polymer synthesis and polymer degradation products, the latter resulting from processes impacting the fibers in the environment (e.g. UV exposure). The three different fiber types were affected differently by exposure to UV corresponding to natural sunlight. PA primarily exhibited changes in surface morphology after 2 months of UV exposure, while the PET and wool fibers reduced surface changes but increased fragmentation into smaller length fibers. All MFs were found to release chemicals that could be identified as degradation products from UV exposure. Furthermore, all MFs contained a range of different additive chemicals, which leached to varying degrees into seawater during exposure as a function of polymer type, additive chemical properties and level of MF degradation. Some additives (e.g. UV stabilizers) rapidly degraded under UV exposure following leaching, and most of the identified polymer degradation products are estimated to quickly biodegrade in natural seawater. However, some of the additive chemicals may be persistent and contribute to the overall chemical pollution load in the oceans.

## CRediT authorship contribution statement

**Lisbet Sørensen:** Conceptualization, Methodology, Validation, Formal analysis, Resources, Writing - original draft, Writing - review &

editing, Visualization, Supervision, Project administration, Funding acquisition. **Anette Synnøve Groven:** Formal analysis, Investigation, Writing - review & editing. **Ingrid Alver Hovsbakken:** Formal analysis, Investigation, Writing - review & editing. **Oihane Del Puerto:** Investigation, Writing - review & editing. **Daniel F. Krause:** Methodology, Formal analysis, Investigation. **Antonio Sarno:** Methodology, Formal analysis, Investigation, Writing - original draft. **Andy M. Booth:** Conceptualization, Validation, Resources, Writing - original draft, Writing - review & editing, Supervision, Funding acquisition.

## Declaration of competing interest

The authors declare that they have no known competing financial interests or personal relationships that could have appeared to influence the work reported in this paper.

## Acknowledgements

Funding was provided by the High North Research Centre for Climate and the Environment (The Fram Centre) (Grant nr. pa092018) and the Norwegian Research Council (Grants nr. 268404, 287939 and 295174). The authors are grateful to Yingdu Ya (NTNU) for SEM imaging, Marianne Molid, Marianne Aas and Lisbet Støen (SINTEF) for experimental assistance. Oihane Del Puerto is grateful to the NoviaSalcedo Fundación, Spain, for financial support.

## Appendix A. Supplementary data

Supplementary data to this article can be found online at https://doi.org/10.1016/j.scitotenv.2020.143170.

## References

Achhammer, B.G., Reinhart, F.W., Kline, G.M., 1951. Mechanism of the degradation of polyamides. J. Appl. Chem. 1, 301–320.

Armstrong, R.D., Jenkins, A.T.A., Johnson, B.W., 1995. An investigation into the uv breakdown of thermoset polyester coatings using impedance spectroscopy. Corrosion Sci. 37, 1615e1625. https://doi.org/10.1016/0010-938X(95)00063-.

Andrady, A.L., 2015. Persistence of plastic litter in the oceans. In: Bergmann, M., Gutow, L., Klages, M. (Eds.), Marine Anthropogenic Litter. Springer International Publishing, Cham, pp. 57–72.

Avagyan, R., Luongo, G., Thorsén, G., Östman, C., 2015. Benzothiazole, benzotriazole, and their derivates in clothing textiles–a potential source of environmental pollutants and human exposure. Environ. Sci. Pollut. Res. Int. 22, 5842–5849.

Ben-David, E.A., Habibi, M., Haddad, E., Hasanin, M., Angel, D.L., Booth, A.M., et al., 2021. Microplastic distributions in a domestic wastewater treatment plant: removal efficiency, seasonal variation and influence of sampling technique. Sci. Total Environ. 752, 141880.

Booth, A.M., Kubowicz, S., Beegle-Krause, C., Skancke, J., Nordam, T., Landsem, E., et al., 2018. Microplastic in Global and Norwegian Marine Environments: Distributions, Degradation Mechanisms and Transport. Norwegian Environment Agency, Trondheim, p. 147. https://www.miljodirektoratet.no/globalassets/publikasjoner/m918/m918.pdf.

Browne, M.A., Crump, P., Niven, S.J., Teuten, E., Tonkin, A., Galloway, T., et al., 2011. Accumulation of microplastic on shorelines worldwide: sources and sinks. Environ. Sci. Technol. 45, 9175–9179.

Buchanan, J.B., 1971. Pollution by synthetic fibres. Mar. Pollut. Bull. 2, 23.

Capolupo, M., Sørensen, L., Jayasena, K.D.R., Booth, A.M., Fabbri, E., 2020. Chemical composition and ecotoxicity of plastic and car tire rubber leachates to aquatic organisms. Water Res. 169, 115270.

Carney Almroth, B.M., Åström, L., Roslund, S., Petersson, H., Johansson, M., Persson, N.-K., 2018. Quantifying shedding of synthetic fibers from textiles; a source of microplastics released into the environment. Environ. Sci. Pollut. Res. 25, 1191–1199.

Cesa, F.S., Turra, A., Checon, H.H., Leonardi, B., Baruque-Ramos, J., 2020. Laundering and textile parameters influence fibers release in household washings. Environ. Pollut. 257, 113553.

Chandure, A.S., Bhusari, G.S., Umare, S.S., 2014. Synthesis, characterization, andbiodegradation studies of poly(1,4-cyclohexanedimethylene-adipate-carbonate) s. J. Polym., 1e11 https://doi.org/10.1155/2014/547325.

Claessens, M., Meester, S.D., Landuyt, L.V., Clerck, K.D., Janssen, C.R., 2011. Occurrence and distribution of microplastics in marine sediments along the Belgian coast. Mar. Pollut. Bull. 62, 2199–2204.

Cole, M., 2016. A novel method for preparing microplastic fibers. Sci. Rep. 6, 34519.

Cole, M., Lindeque, P., Fileman, E., Halsband, C., Goodhead, R., Moger, J., et al., 2013. Microplastic ingestion by zooplankton. Environ. Sci. Technol. 47, 6646–6655.

Cole, M., Coppock, R., Lindeque, P.K., Altin, D., Reed, S., Pond, D.W., et al., 2019. Effects of nylon microplastic on feeding, lipid accumulation, and Moulting in a Coldwater copepod. Environ. Sci. Technol. 53, 7075–7082.

De Falco, F., Gullo, M.P., Gentile, G., Di Pace, E., Cocca, M., Gelabert, L., et al., 2018. Evaluation of microplastic release caused by textile washing processes of synthetic fabrics. Environ. Pollut. 236, 916–925.

Dsikowitzky, L., Nordhaus, I., Sujatha, C.H., Akhil, P.S., Soman, K., Schwarzbauer, J., 2014. A combined chemical and biological assessment of industrial contamination in an estuarine system in Kerala, India. Sci. Total Environ. 485-486, 348–362.

Fechine, G.J.M., Rabello, M.S., Souto Maior, R.M., Catalani, L.H., 2004. Surface characterization of photodegraded poly(ethylene terephthalate). The effect of ultraviolet absorbers. Polymer 45, 2303–2308.

Freeman, S., Booth, A.M., Sabbah, I., Tiller, R., Dierking, J., Klun, K., et al., 2020. Between source and sea: the role of wastewater treatment in reducing marine microplastics. J. Environ. Manag. 266, 110642.

Frias, J., Nash, R., 2019. Microplastics: finding a consensus on the definition. Mar. Pollut. Bull. 138, 145–147.

Gewert, B., Plassmann, M., Sandblom, O., MacLeod, M., 2018. Identification of chain scission products released to water by plastic exposed to ultraviolet light. Environ. Sci. Technol. Lett. 5, 272–276.

Habib, D., Locke, D.C., Cannone, L.J., 1998. Synthetic fibers as indicators of municipal sewage sludge, sludge products, and sewage treatment plant effluents. Water Air Soil Pollut. 103, 1–8.

Hartline, N.L., Bruce, N.J., Karba, S.N., Ruff, E.O., Sonar, S.U., Holden, P.A., 2016. Microfiber masses recovered from conventional machine washing of new or aged garments. Environ. Sci. Technol. 50, 11532–11538.

Hermabessiere, L., Dehaut, A., Paul-Pont, I., Lacroix, C., Jezequel, R., Soudant, P., et al., 2017. Occurrence and effects of plastic additives on marine environments and organisms: a review. Chemosphere 182, 781–793.

Imbert, L., Saussereau, E., Lacroix, C., 2014. Analysis of eight glycols in serum using LC-ESI–MS-MS. J. Anal. Toxicol. 38, 676–680.

Jemec, A., Horvat, P., Kunej, U., Bele, M., Kržan, A., 2016. Uptake and effects of microplastic textile fibers on freshwater crustacean Daphnia magna. Environ. Pollut. 219, 201–209.

Kanhai, L.D., Gardfeldt, K., Thompson, R.C., O'Connor, I., 2018. An investigation of microplastic contamination in the Arctic Central Basin. In: Baztan, J.B.M., Carrasco, A., Fossi, C., Jorgensen, B., Miguelez, Q., Pahl, S., Thompson, R.C., Vanderlinden, J.-P. (Eds.), MICRO2018. Fate and Impact of Microplastics: Knowledge, Actions and Solutions., Lanzarote.

Lares, M., Ncibi, M.C., Sillanpää, M., Sillanpää, M., 2018. Occurrence, identification and removal of microplastic particles and fibers in conventional activated sludge process and advanced MBR technology. Water Res. 133, 236–246.

Leslie, H.A., Brandsma, S.H., van Velzen, M.J.M., Vethaak, A.D., 2017. Microplastics en route: field measurements in the Dutch river delta and Amsterdam canals, wastewater treatment plants, North Sea sediments and biota. Environ. Int. 101, 133–142.

Liu, W., Xue, J., Kannan, K., 2017. Occurrence of and exposure to benzothiazoles and benzotriazoles from textiles and infant clothing. Sci. Total Environ. 592, 91–96.

Lock, L.M., Frank, G.C., 1973. A study of some factors affecting the Photodegradation of textile yarns part II: nylon 66 and polyethylene terephthalate yarns. Text. Res. J. 43, 502–512.

Luongo, G., Avagyan, R., Hongyu, R., Östman, C., 2016. The washout effect during laundry on benzothiazole, benzotriazole, quinoline, and their derivatives in clothing textiles. Environ. Sci. Pollut. Res. Int. 23, 2537–2548.

Lusher, A.L., Tirelli, V., O'Connor, I., Officer, R., 2015. Microplastics in Arctic polar waters: the first reported values of particles in surface and sub-surface samples. Sci. Rep. 5, 14947.

Mathalon, A., Hill, P., 2014. Microplastic fibers in the intertidal ecosystem surrounding Halifax Harbor, Nova Scotia. Mar. Pollut. Bull. 81, 69–79.

Napper, I.E., Thompson, R.C., 2016. Release of synthetic microplastic plastic fibres from domestic washing machines: effects of fabric type and washing conditions. Mar. Pollut. Bull. 112, 39–45.

Nerland, I.L., Halsband, C., Allan, I., Thomas, K.V., 2014. Microplastics in Marine Environments: Occurrence, Distribution and Effects. Norwegian Institute for Water Research, p. 71.

Obbard, R.W., Sadri, S., Wong, Y.Q., Khitun, A.A., Baker, I., Thompson, R.C., 2014. Global warming releases microplastic legacy frozen in Arctic Sea ice. Earth's Future 2, 315–320.

R Development Core Team, 2008. R: A language and environment for statistical computing. R Foundation for Statistical Computing, from http://www.R-project.org.

Rummel, C.D., Escher, B.I., Sandblom, O., Plassmann, M.M., Arp, H.P.H., MacLeod, M., et al., 2019. Effects of Leachates from UV-weathered microplastic in cell-based bioassays. Environ. Sci. Technol. 53 (15), 9214–9223.

Sait, S.T.L., Sørensen, L., Kubowicz, S., Vike-Jonas, K., Gonzalez, S.V., Asimakopoulos, A.G., et al., 2020. Microplastic fibres from synthetic textiles: environmental degradation and additive chemical content. Environ. Pollut. 115745.

Salvador Cesa, F., Turra, A., Baruque-Ramos, J., 2017. Synthetic fibers as microplastics in the marine environment: a review from textile perspective with a focus on domestic washings. Sci. Total Environ. 598, 1116–1129.

Sathish, N., Jeyasanta, K.I., Patterson, J., 2019. Abundance, characteristics and surface degradation features of microplastics in beach sediments of five coastal areas in Tamil Nadu, India. Mar. Pollut. Bull. 142, 112–118.

Schneider, C.A., Rasband, W.S., Eliceiri, K.W., 2012. NIH image to ImageJ: 25 years of image analysis. Nat. Methods 9, 671.

Sørensen, L., Rogers, E., Altin, D., Salaberria, I., Booth, A.M., 2020. Sorption of PAHs to microplastic and their bioavailability and toxicity to marine copepods under co-exposure conditions. Environ. Pollut. 258, 113844.
Thompson, R.C., Olsen, Y., Mitchell, R.P., Davis, A., Rowland, S.J., John, A.W.G., et al., 2004. Lost at sea: where is all the plastic? Science 304, 838.
Tokiwa, Y., Calabia, B.P., Ugwu, C.U., Aiba, S., 2009. Biodegradability of plastics. Int. J. Mol. Sci. 10, 3722–3742.
US EPA, 2012. Estimation Programs Interface Suite™ for Microsoft® Windows. United States Environmental Protection Agency (US EPA), Washington, DC, USA.
Zhang, H., Wang, J., Zhou, B., Zhou, Y., Dai, Z., Zhou, Q., et al., 2018. Enhanced adsorption of oxytetracycline to weathered microplastic polystyrene: kinetics, isotherms and influencing factors. Environ. Pollut. 243, 1550–1557.
Zimmermann, L., Dierkes, G., Ternes, T.A., Völker, C., Wagner, M., 2019. Benchmarking the in vitro toxicity and chemical composition of plastic consumer products. Environ. Sci. Technol. 53, 11467–11477.